Acta Biomaterialia xxx (2011) xxx–xxx

Contents lists available at ScienceDirect

Acta Biomaterialia

journal homepage: www.elsevier.com/locate/actabiomat

Brief communication

Anodic mesoporous TiO_2 layer on Ti for enhanced formation of biomimetic hydroxyapatite

Tuli Dey [a,b], Poulomi Roy [a], Ben Fabry [b], Patrik Schmuki [a,*]

[a] Department of Materials Science, WW4-LKO, University of Erlangen-Nuremberg, Martensstrasse 7, D-91058 Erlangen, Germany
[b] Center for Medical Physics and Technology, Department of Physics, University of Erlangen-Nuremberg, Henkestrasse 91, 91052 Erlangen, Germany

ARTICLE INFO

Article history:
Received 24 September 2010
Received in revised form 3 November 2010
Accepted 8 November 2010
Available online xxxx

Keywords:
TiO_2
Mesopores
Hydroxyapatite
Simulated body fluid
Anodization

ABSTRACT

Ti surfaces can be very efficiently coated by a robust (μm thick) mesoporous titania layer (MTL). These coatings are produced by anodization of Ti at elevated temperature in a glycerol/K_2HPO_4 electrolyte, followed by an appropriate etching process. In the present work we examine these layers with regard to their ability to form hydroxyapatite. Immersion tests in two types of simulated body fluids (Kokubo SBF and Bohner and Lemaitre SBF) combined with scanning electron microscopy, X-ray diffraction and X-ray photoelectron spectroscopy investigations show that these MTL layers lead to a significant enhancement of HAp formation and anchoring in the structure compared with non-coated or even nanotubular Ti surface coatings (these were recently reported to be the most efficient in terms of HAp formation).

1. Introduction

Titanium and its alloys have over the past few decades become the premier choice for "biocompatible" dental and hip replacement implant materials [1,2]. Implant–bone integration and long-term stability of the implant are mainly found to be influenced by the initial osseogenesis, which largely depends on the nature (chemistry and topography) of the implant surface. Bioactivity or the bone bonding capacity of implant surfaces [3] is frequently quantified by their ability to form bone-like apatite in vitro [4]. For this various versions of simulated body fluids (SBFs), metastable calcium phosphate solutions, have frequently been used to assess the amount and quality of apatite formed with time.

Numerous approaches have been reported to improve bone–implant contact, changing the implant surface topography or chemically modifying the surface layer (e.g. sandblasting, etching in acid or alkaline solutions, or creating optimized surface layers by various deposition techniques [5–7] and a range of modification approaches). It should be noted, however, that metallic Ti implant surfaces, in any applied form, are covered by a thin native oxide film.

TiO_2 surface modifications have been extensively studied in view of their osseointegrative behaviour. One of the most explored techniques to improve the osseointegrative properties is electrochemical anodization of the metal surface to form various morphologies of TiO_2 layers. A frequently used approach is spark anodization, in which, by applying a sufficiently high voltage, dielectric breakdown of the oxide layer is triggered, leading to a roughened surface morphology. Such layers were shown to have enhanced bone in-growth properties [8–10]. Another promising electrochemical approach is the anodization of Ti metal in a HF-containing electrolyte to form self-organized TiO_2 nanotubes. Such a nanotubular structure was found to be very efficient for hydroxyapatite formation compared with compact oxide layers [11–14]. The most effective enhancement of HAp formation was found if the nanotubes had an anatase structure. Further enhancement of HAp formation on nanotube layers was obtained by using an alternate dipping approach [15] to create HAp nucleation centres within the tubes [14].

Although such nanotubular structures show higher and efficient HAp formation, longer nanotubes were found to be mechanically unstable [16] and this may compromise the implant behaviour in vivo. Recently, a novel anodic TiO_2 nanostructural layer was reported [16–19], composed of nano-channels and showing a much higher mechanical stability. This mesoporous titania layer (MTL) reportedly has a higher surface area and better adheres to the Ti substrate under stress [16]. In the present study we investigated the bioactivity of this nano-channel surface in the light of its HAp formation ability. Apart from the kinetics, the structure and chemical composition of HAp obtained from two standard SBFs were also compared with the results from the (up to now) most efficient nanotubular system.

* Corresponding author. Tel.: +49 9131 852 7575; fax: +49 9131 852 7582.
E-mail address: schmuki@ww.uni-erlangen.de (P. Schmuki).

1742-7061/$ - see front matter © 2010 Acta Materialia Inc. Published by Elsevier Ltd. All rights reserved.
doi:10.1016/j.actbio.2010.11.011

2. Materials and methods

2.1. Fabrication of titania meso-sponge and nanotube layers

A MTL and titania nanotubes were prepared from 0.1 mm thick Ti foil (99.9% purity) which was cleaned by immersion in acetone, methanol and distilled water. To prepare an approximately 10 μm thick MTL structure, anodization of the Ti foil was carried out at 1 V in dehydrated glycerol/K_2HPO_4 solution at 180 °C for 3 h in a two electrode system [16,19]. The samples then were cleaned by overnight washing in distilled water and dried in a N_2 stream. For etching treatments the anodized samples were sonicated in 30 wt.% H_2O_2 in a sonication bath for 1 h at room temperature. After treatment the samples were rinsed with deionized water and dried in a nitrogen stream.

Nanotubular arrays were grown on the Ti foil by anodization at 10 V for 2 h in a 1 M H_3PO_4 (Merck) solution with the addition of 0.3 wt.% HF (Merck) [20]. Anodization was performed in an electrochemical cell with a three electrode configuration, with Ti foil as the working electrode, platinum gauze as the counter electrode and a Haber–Luggin capillary containing Ag/AgCl (1 M KCl) electrode as the reference electrode. The samples were washed with deionized water and dried with a stream of N_2. The thickness of the nanotubular array was found to be approximately 1 μm, with a tube diameter of 50 nm. Some reference experiments were carried out using compact anodic oxides fabricated according to Tsuchiya et al. [11].

Annealing of samples was carried out in a Rapid Thermal Annealer (Jipelec JetFirst100) at 450 °C in air at a heating and cooling rate of 30 °C min^{-1} to convert the as-formed layer into anatase/rutile phase.

2.2. Apatite growth

In order to investigate the formation of apatite on the different TiO_2 samples we used two different compositions of SBF: (i) the classic Kokubo solution [21] and (ii) a modified solution proposed by Bohner and Lemaitre [22]. Briefly the Kokubo ($_K$SBF) solution with ionic concentrations equal to human blood plasma was prepared by sequentially dissolving reagent grade chemicals, including NaCl, KCl, $NaHCO_3$, $MgSO_4{\cdot}12H_2O$, $CaCl_2$, and KH_2PO_4, in double distilled water at 37 °C and buffered with TRIS and HCl at ~pH 7.4. The chemical composition is as follows (mmol l^{-1}): Na^+, 142.0; K^+, 5.0; Mg^{2+}, 1.0; Ca^{2+}, 2.5; Cl^-, 131.0; HCO_3^-, 5.0; HPO_4^{2-}, 1.0; SO_4^{2-}, 1.0 [23,24]. The Bohner and Lemaitre solution ($_c$SBF3) was prepared as in Bohner and Lemaitre [22]. To induce HAp growth 1 cm^2 samples were soaked in the 50 ml cm^{-2} SBF solution under static conditions in a biological thermostat at 37 °C for different durations (in days). After the experiment the samples were rinsed with 20 ml of deionized water and dried at 60 °C for 1 h.

2.3. Characterization of surface morphology, structure and chemical composition

The surface morphology after anodization and SBF soaking was characterized by field emission scanning electron microscopy (FE-SEM) using a Hitachi FE-SEM S4800 equipped for energy dispersive

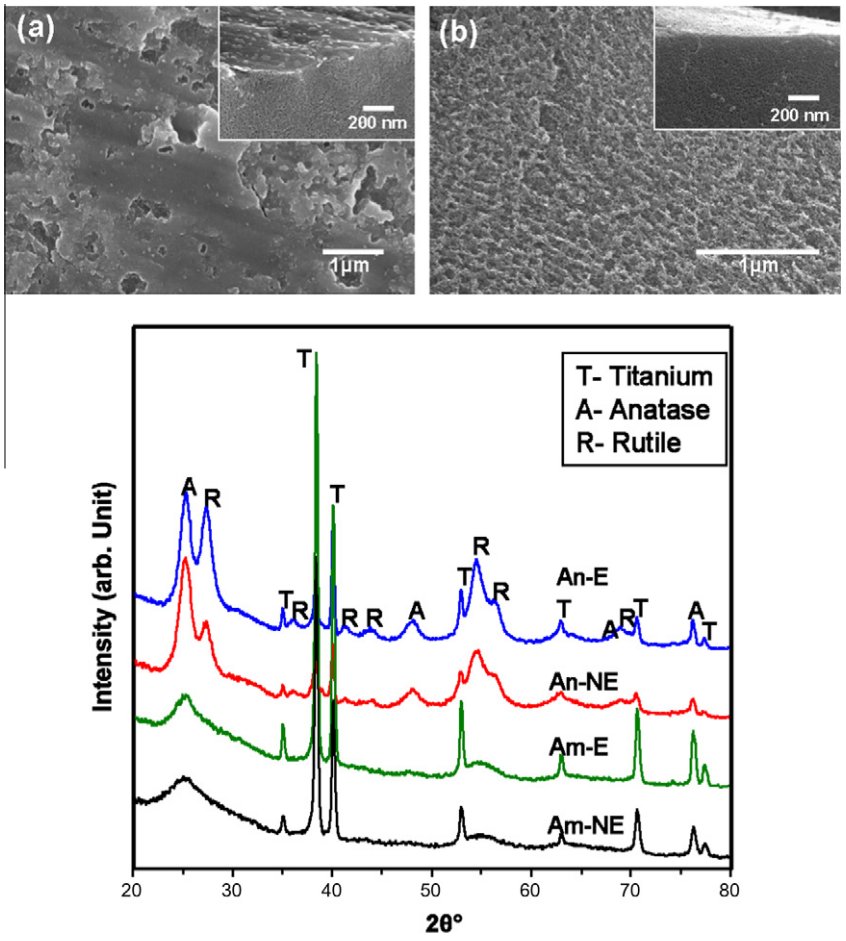

Fig. 1. SEM images of cross-sectional (inset: top) views of (a) the as-formed (non-etched) mesoporous titania (MTL) layer showing the presence of a thin top layer and (b) the MTL layer after etching in H_2O_2 solution. (c) XRD patterns of the MTL layers after different annealing and etching treatments. Am-NE, amorphous non-etched; Am-E, amorphous etched; An-NE, annealed non-etched; An-E, annealed etched.

Please cite this article in press as: Dey T et al. Anodic mesoporous TiO_2 layer on Ti for enhanced formation of biomimetic hydroxyapatite. Acta Biomater (2011), doi:10.1016/j.actbio.2010.11.011

X-ray (EDX) analysis. Phase identification of the surface was carried out with an X-ray diffractometer (Phillips X'Pert-MPD PW-3040, Siemens Kristalloflex D 500) with an incident beam of 1.54060 Å wavelength.

XPS spectra were recorded using Alk_α radiation (1486.6 eV) as the excitation source. The take-off angle θ of the emitted photoelectrons was adjusted to 45° with respect to the surface normal. The binding energies of the target elements (Ti 2*p*, O 1*s*, F 1*s*, C 1*s*, P 2*p*, N 1*s*, Ca 2*p*, K 2*p*, and Mg 2*p*) were determined at a pass energy of 23.5 eV, with a resolution of 0.1 eV, using the binding energy of carbon (C 1*s* = 284.8 eV) as a reference.

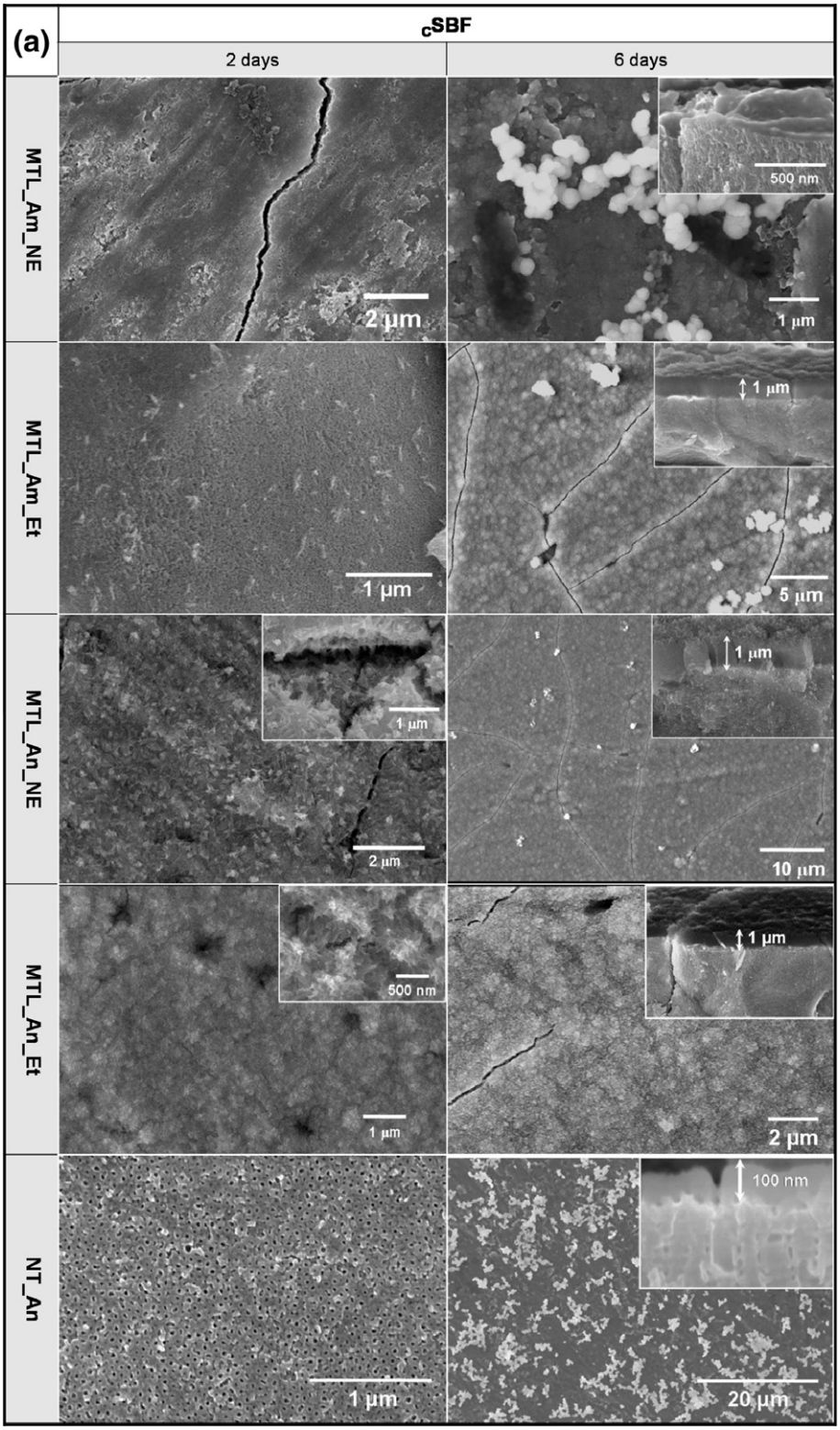

Fig. 2. Compilation SEM characterization of HAp formation on different MTL surfaces as well as TiO_2 nanotube surfaces for different immersion times in (a) $_c$SBF3 and (b) $_K$SBF solutions. Am-NE, amorphous non-etched; Am-E, amorphous etched; An-NE, annealed non-etched; An-E, annealed etched; NT nanotubes.

Please cite this article in press as: Dey T et al. Anodic mesoporous TiO_2 layer on Ti for enhanced formation of biomimetic hydroxyapatite. Acta Biomater (2011), doi:10.1016/j.actbio.2010.11.011

3. Results and discussion

The morphology of 10 μm thick MTL layers fabricated by electrochemical anodization is shown in Fig. 1a. It is apparent that the entire oxide layer after formation consists of interlinked regular channels of 8–12 nm diameter. However, for the "as-formed" layer a thin, dense surface layer is present on top of the open channels. In order to remove this layer and to widen the channels an etching treatment in H_2O_2 was carried out as described above. After treatment the morphology shown in Fig. 1b was obtained. Clearly, the top layer had been removed and the channels were approximately 12 nm in diameter. XRD investigations of the MTL before and after etching show the layers to be mostly amorphous, but they contain some anatase and rutile phase (Fig. 1c). These

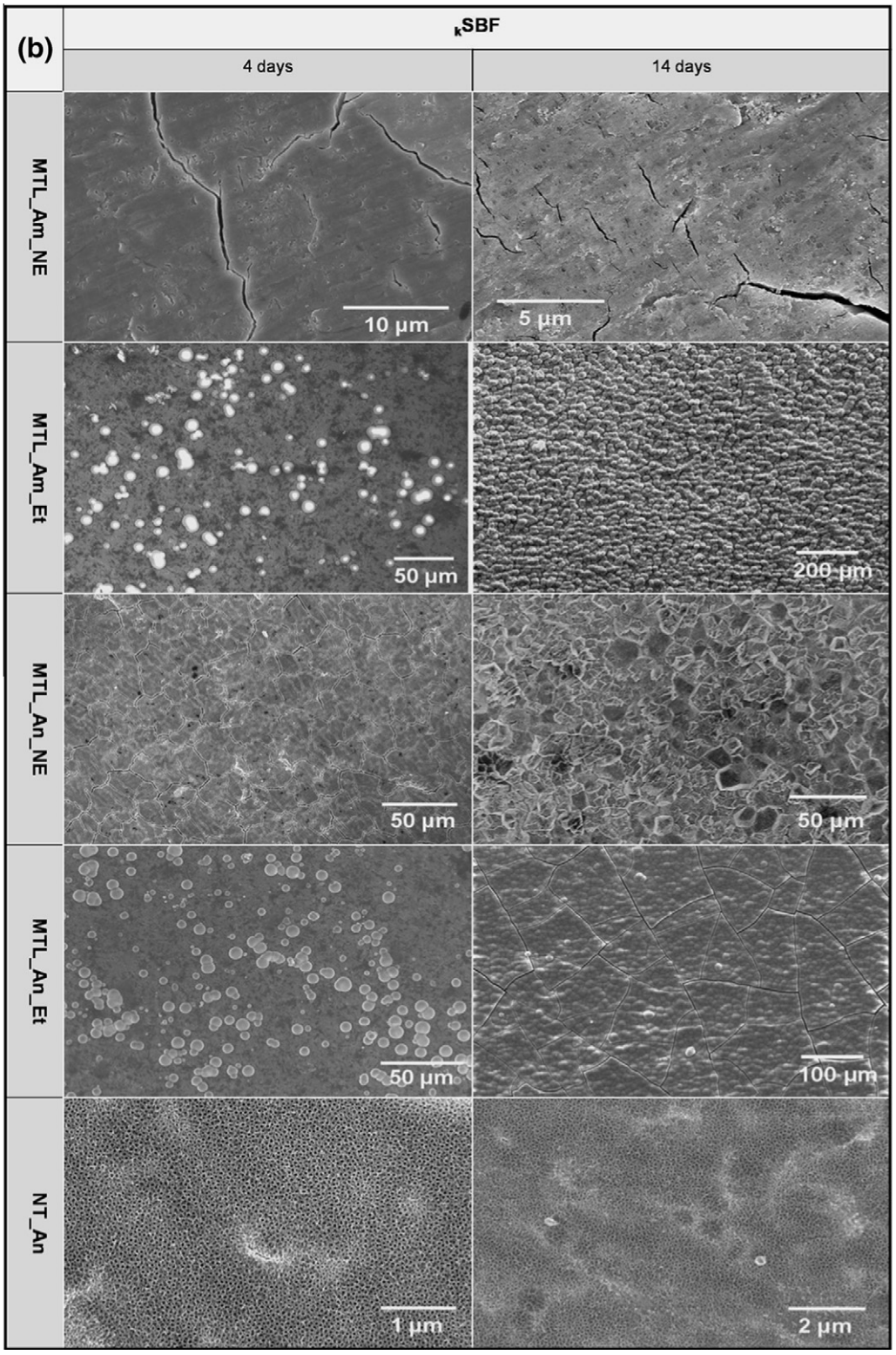

Fig. 2 (*continued*)

Please cite this article in press as: Dey T et al. Anodic mesoporous TiO_2 layer on Ti for enhanced formation of biomimetic hydroxyapatite. Acta Biomater (2011), doi:10.1016/j.actbio.2010.11.011

partially crystalline MTL layers can be fully crystallized into a mixture of anatase and rutile by annealing at 450 °C for 3 h in air (Fig. 1c).

The as-formed and annealed layers were then used in immersion tests in the two different SBFs. In order to compare the results with previous work we used as a reference compact oxide samples and, as a "gold-standard", a nanotube layer previously reported to significantly accelerate HAp formation [11–13]. Incubation in different SBFs for different time periods (6 and 14 days) was used based on the literature [11] and the estimated differences in HAp precipitation rates. Fig. 2 shows a compilation of the surface morphology after HAp formation on the different MTL and nanotube layers in the two SBF solutions. The MTL layers (after etching and etched and annealed) clearly show the highest coverage for the $_{c}$SBF3 solution (Fig. 2a), with a complete 1 μm thick layer after 6 days. The amorphous non-etched and only etched MTL layers show significantly less HAp formation after 2 and 6 days. The best surface, etched anatase MTL, shows HAp formation over the entire surface after 2 days. In comparison, on anatase nanotubes, although HAp formation could be observed after 2 days, a thickness of only ~100 nm of HAp was achieved at some locations, even after 6 days.

If $_{K}$SBF solution is used (Fig. 2b) HAp formation can only be observed in the case of etched MTL samples (amorphous as well as anatase) after 4 days and the highest growth rate is clearly obtained on the etched and annealed surface. In comparison with $_{c}$SBF3 (0.4 mg day^{-1}), $_{K}$SBF leads to much slower HAp formation (0.16 mg day^{-1}), however, after 14 days a thick layer completely covering the surface can be observed for the MTL. The etched anatase MTL layer shows better coverage by HAp compared with an etched amorphous MTL layer. As in the case of $_{c}$SBF3, anatase TiO_2 nanotubes show comparably much less precipitation even after 14 days. Morphologically, HAp formation in the two different solutions is different. In $_{K}$SBF solution globular HAp was observed on MTL, forming large plates over the entire surface after 14 days incubation. This visibly resembles previously reported structures of crystalline HAp on nanotube surfaces [11]. In contrast, in $_{c}$SBF3 a rather spongy morphology of the HAp precipitate can be observed, which is intuitively in line with very fast HAp formation. In spite of the observed differences for the two SBF solutions, the general trend of Hap formation remains the same, i.e. the etched, annealed MTL surface always shows the most efficient HAp formation (more efficient than nanotubes). Such layers trigger HAp formation even faster than nanotubular layers, which were previously reported to show the most beneficial effect. In both solutions no significant HAp formation could be observed after the maximum test time for reference samples of compact oxides, in line with earlier observations by Tsuchiya et al. [11].

In order to provide a quantitative comparison between the various TiO_2 surfaces and the two different SBF solutions the mass gain during HAp formation was evaluated (Fig. 3). These results confirm the SEM observations, i.e. that the etched anatase MTL layers are the most efficient surface for HAp formation in comparison not only with other forms of MTL but also compared with nanotubular surfaces. Nevertheless, a significant and important difference between the two SBF solutions can be seen in Fig. 4. Excellent in-growth of HAp into the porous matrix is observed for the MTL layer

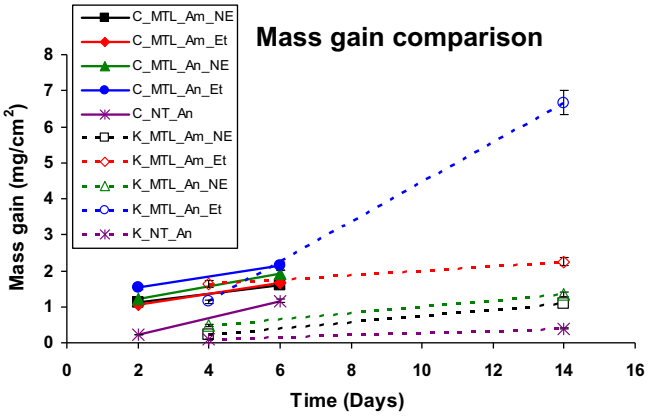

Fig. 3. Mass gain of the samples after HAp loading for different durations in $_{c}$SBF3 and $_{K}$SBF solutions. Am-NE, amorphous non-etched; Am-Et, amorphous etched; An-NE, annealed non-etched; An-Et, annealed etched; NT, nanotubes; C, $_{c}$SBF3 solution; K, $_{K}$SBF solution.

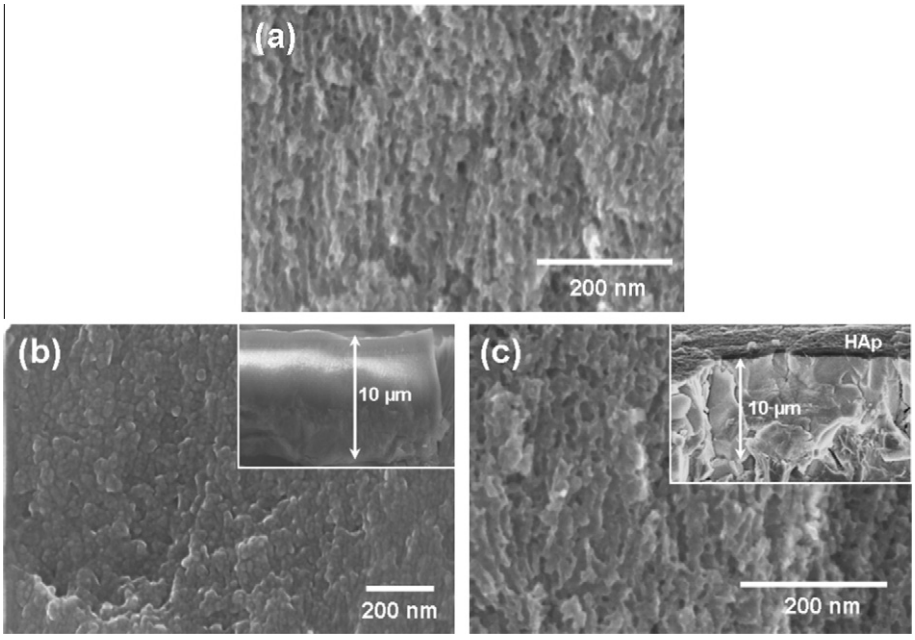

Fig. 4. Comparison of in-growth HAp formation in etched anatase MTL layers: cross-sectional SEM images of MTL layers (a) before and (b and c) after soaking in (b) $_{K}$SBF and (c) $_{c}$SBF3 solutions after 6 and 14 days, respectively. For $_{K}$SBF the pores are filled with HAp (complete in-growth); for $_{c}$SBF3 only a top layer is formed.

Please cite this article in press as: Dey T et al. Anodic mesoporous TiO_2 layer on Ti for enhanced formation of biomimetic hydroxyapatite. Acta Biomater (2011), doi:10.1016/j.actbio.2010.11.011

after 14 days in $_K$SBF solution, whereas in $_c$SBF3 solution HAp precipitation occurs only on the top layer (Fig. 4c).

For HAp layers formed from both the $_c$SBF3 and $_K$SBF solutions after 6 and 14 days, respectively, XPS analysis (Fig. 5) reveals a similar overall composition. Both apatite layers show traces of magnesium and sodium in addition to the main components calcium and phosphorus. Mg^{2+} and Na^+ ions might substitute Ca ions in apatites, which is in line with the composition of biological apatites from human bones, which is non-stoichiometric. Traces of ions such as Mg^{2+} and Na^+, as well as the anions CO_3^{2-}, HPO_4^{2-}, F^-, and Cl^-, are also present in natural apatite. A qualitative analysis shows that the composition of the apatite layers, in particular the Ca/P ratio, are close to physiological Hap, as shown in Fig. 5d (EDX results are also included). Physiological apatite has a Ca:P ratio of 1.35–1.46 [25], thus it may be noteworthy that apatite formed from $_K$SBF solution has somewhat lower Ca to P ratio. The nature of the apatite forming substrate, however, amorphous or annealed, or the morphology, channel or tubular structure (compare the results in Tsuchiya et al. [11]), do not seem to influence the final composition of the apatite.

Fig. 6 shows XRD patterns of the HAp layers on the etched anatase MTL surface after 6 and 14 days soaking in $_c$SBF3 and $_K$SBF solution, respectively. The XRD pattern of the HAp layer grown in $_c$SBF3 solution shows peaks corresponding to anatase TiO_2 as well as a small peak at ~32° for HAp, whereas the HAp layer grown in $_K$SBF solution only shows peaks corresponding to HAp. This difference is due to the morphological difference in HAp formation in the two different solutions as well as the in-growth phenomena of HAp

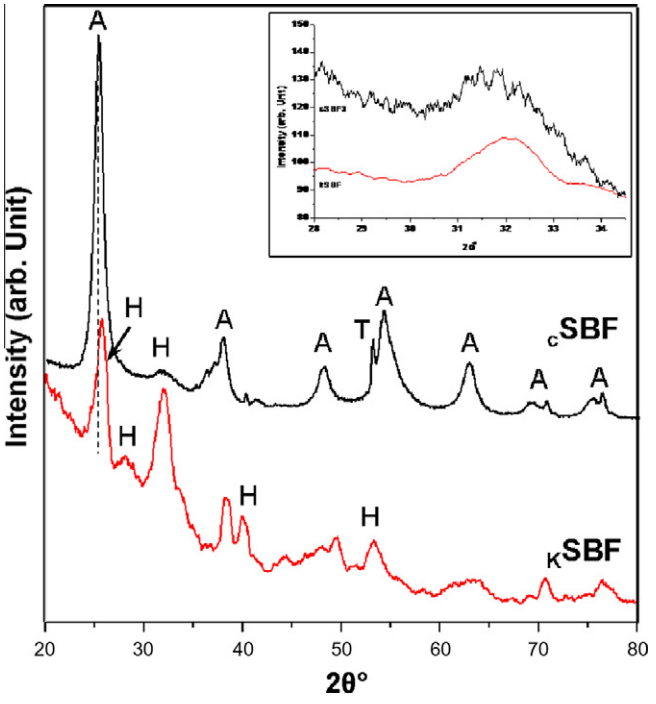

Fig. 6. XRD pattern of HAp layers grown on the etched anatase MTL layer in $_c$SBF3 and $_K$SBF solution after 6 and 14 days, respectively. H, HAp; A, anatase TiO_2. (Inset) Magnified XRD pattern near the characteristic HAp peak at 32°.

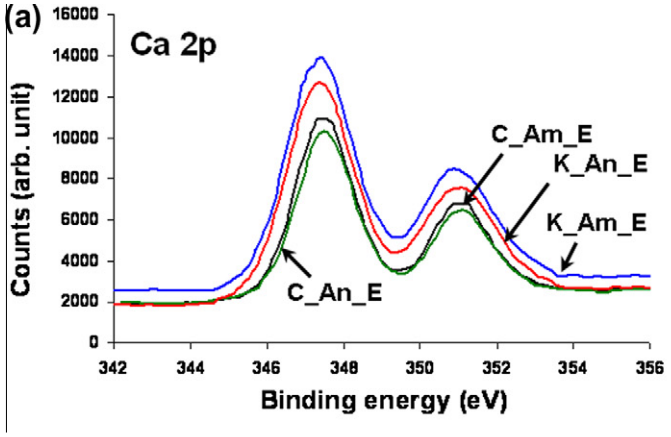

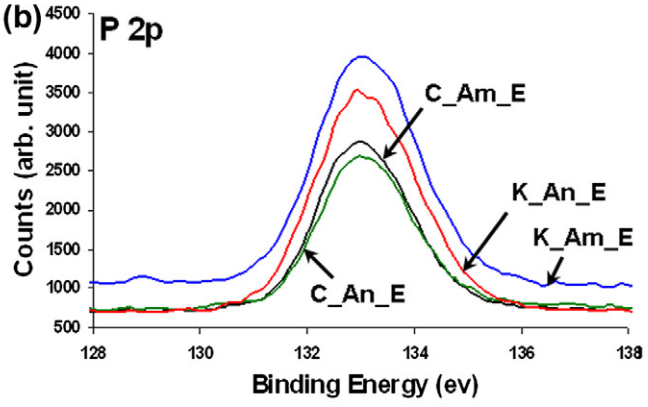

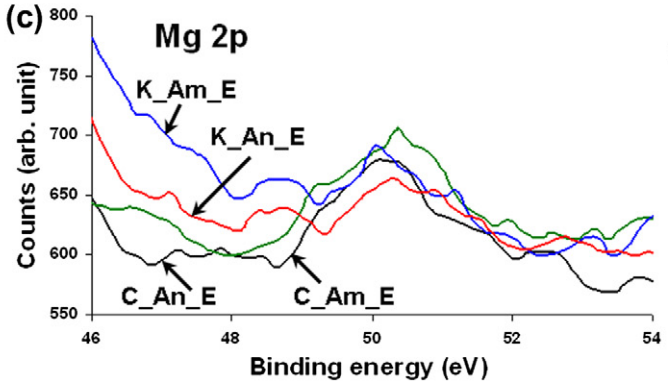

(d)

Sample		Ca / P	
		EDX	XPS
$_c$SBF	Am_Et_D6	1.41	1.40
	An_Et_D6	1.42	1.47
$_K$SBF	Am_Et_D14	1.35	1.32
	An_Et_D14	1.37	1.36

Fig. 5. (a–c) XPS of the Ca 2*p*, P 2*p* and Mg 2*p* peaks recorded from the HAp layers grown on the different MTL surfaces and in the different SBF solutions (in $_c$SBF3 after day 6 and $_K$SBF after day 14). (d) Ca/P ratios of HAp grown on different MTL surfaces in different solutions calculated from the XPS and EDX analysis. Abbreviations are as in the previous figures.

Please cite this article in press as: Dey T et al. Anodic mesoporous TiO_2 layer on Ti for enhanced formation of biomimetic hydroxyapatite. Acta Biomater (2011), doi:10.1016/j.actbio.2010.11.011

in the $_K$SBF solution. The magnified XRD pattern at ~32° (inset of Fig. 6) shows that both HAp layers are similar in terms of crystallinity. The main reflections of crystalline HAp originate from the (2 1 1) plane at 31.87°, the (1 1 2) plane at 32.18°, and the (3 0 0) plane at 32.87°. The diffraction line at 26°, in the case of $_K$SBF solution, corresponds to reflection from the (0 0 2) plane of HAp. However, in case of $_c$SBF3 solution this weak peak overlaps with the sharp anatase peak from the substrate. These results are very well in line with previous work on compact TiO_2 layers and HAp formed on TiO_2 nanotubes [11]; in other words, the HAp formed on MTL layers is typical HAp (in structure and chemistry), as formed on other TiO_2 surfaces, only the growth is significantly stimulated (if conditioned to a crystalline and open structure).

As already discussed for nanotubes, one major point in the growth stimulating effect may be the microscopic roughness (acting as nucleation sites) provided by these nanostructures, combined with suppression of conventional agitation within the nanochannels. Although the origin of this beneficial effect is not entirely clear, the present work shows that MTL layers may be a very promising candidate as a biomedical implant coating due to the stimulating effect on HAp formation of this titania surface.

4. Conclusions

In conclusion, we report a mesoporous titania layer that acts as an efficient surface for HAp growth from SBF. We show that the layers need to be etched to provide open channels and should be annealed to be most efficient. Such layers trigger HAp formation even faster than the previously reported most beneficial nanotubular layers. We demonstrate that the acceleration effect holds for two different SBF solutions ($_K$SBF and $_c$SBF3), with HAp precipitation from $_K$SBF solution being slower than from $_c$SBF3 solution. The chemical composition of the HAp formed in the two different solutions shows some slight variations in the Ca/P ratio, although for both solutions it is in the range of physiological HAp. A most important effect is that in $_K$SBF efficient in-growth of HAp into the porous TiO_2 layer is observed. This may be ascribed to the slower crystallization rate of the $_K$SBF solution. This point may be of very high practical significance, as it suggests that with these layers better anchorage of HAp to the substrate can be achieved. Overall, the novel MTL coating for Ti surfaces presented here is a promising (easy, cheap and applicable to various geometries), and seems in many respects to be superior to previously reported (highly active) nanotubular coatings.

Acknowledgements

The authors acknowledge Helga Hildebrand for the XPS analysis. We thank the DFG and the DFG Cluster of Excellence for their financial support.

Appendix Appendix. Figures with essential colour discrimination

Certain figures in this article, particularly Figs. 1, 3, 5 and 6, are difficult to interpret in black and white. The full colour images can be found in the on-line version, at doi:10.1016/j.actbio.2010.11.011.

References

[1] Branemark PI, Hansson, Adell R, Breine U, Lindstrom J, Hallen O, et al. Osseointegrated implants in the treatment of the edentulous jaw. Experience from a 10 year period. Scand J Plast Recontsr Surg 1977;11:39.
[2] Brunette DM, Tengvall P, Textor M, Thomsen P, editors. Titanium in medicine. Berlin: Springer; 2001.
[3] Williams DF, editor. Definitions in biomaterials. Amsterdam: Elsevier; 1987.
[4] Kokubo T, Takadama H. How useful is SBF in predicting in vivo bone bioactivity? Biomaterials 2006;27:2907–15.
[5] Wisbey A, Gregson PJ, Peter LM, Tuke M. Effect of surface treatment on the dissolution of titanium based implant materials. Biometrials 1991;12:470–3.
[6] Zhu X, Eibl O, Scheideler L, Geis-Gerstorfer J. Characterization of nano hydroxyapatite/collagen surfaces and cellular behaviors. J Biomed Mater Res A 2006:114–27.
[7] Xiao SJ, Kenausi G, Textor M. Biochemical modification of titanium surfaces. In: Brunette DM, Tengvall P, Textor M, Thomsen P, editors. Titanium in medicine. Berlin: Springer; 2001. p. 417–55.
[8] Yang B, Uchida M, Kim HM, Zhang X, Kokubo T. Preparation of bioactive titanium metal via anodic oxidation treatment. Biomaterials 2004;25:1003–10.
[9] Sul YT, Johansson CB, Petronis S, Krozer A, Jeong Y, Wennerberg A, et al. Characteristics of the surface oxides on turned and electrochemically oxidized pure titanium implants up to dielectric breakdown: The oxide thickness, micropore configuration, surface roughness, crystal structure and chemical composition. Biomaterials 2002;23:491–501.
[10] Song WH, Jun YK, Han Y, Hong SH. Biomimetic apatite coatings on micro-acr oxidized titania. Biomaterials 2004;25:3341–9.
[11] Tsuchiya H, Macak JM, Muller L, Kunze J, Muller F, Greil P, et al. Hydroxyapatite growth on anodic TiO_2 nanotubes. J Biomed Mater Res A 2006;77:534–41.
[12] Kunze J, Müller L, Macak JM, Greil P, Schmuki P, Müller FA. Time-dependent growth of biomimetic apatite on anodic TiO_2 nanotubes. Electrochim Acta 2008;53:6995–7003.
[13] Oh S-H, Finones RR, Daraio C, Chen L-H, Jin S. Growth of nano-scale hydroxyapatite using chemically treated titanium oxide nanotubes. Biomaterials 2005;26:4938–43.
[14] Kodama A, Bauer S, Komatsu A, Asoh H, Ono S, Schmuki P. Bioactivation of titanium surfaces using coatings of TiO_2 nanotubes rapidly pre-loaded with synthetic hydroxyapatite. Acta Biomater 2009;5:2322–30.
[15] Ono S, Kiyotake A, Asoh H. Effect of nanostructured surfaces of light metals on hydroxyapatite coating. ECS Trans 2008;11(15):1–8.
[16] Kim D, Lee K, Roy P, Birajdar BI, Spiecker E, Schmuki P. Formation of a non-thickness-limited titanium dioxide mesosponge and its use in dye-sensitized solar cells. Angew Chem Int Ed 2009;48:9326–9.
[17] Lee K, Kim D, Roy P, Paramasivam I, Birajdar BI, Spiecker E, et al. Anodic formation of thick anatase TiO_2 mesosponge layers for high-efficiency photocatalysis. J Am Chem Soc 2010;132:1478–9.
[18] Kim D, Roy P, Lee K, Schmuki P. Dye-sensitized solar cells using anodic TiO_2 mesosponge: improved efficiency by $TiCl_4$ treatment. Electrochem Commun 2010;12:574–8.
[19] Roy P, Dey T, Lee K, Kim D, Fabry B, Schmuki P. Size-selective separation of macromolecules by nanochannel titania membrane with self-leaning (declogging) ability. J Am Chem Soc 2010;132:7893–5.
[20] Bauer S, Kleber S, Schmuki P. TiO_2 nanotubes: tailoring the geometry in H_3PO_4/HF electrolytes. Electrochem Commun 2006;8:1321–5.
[21] Kokubo T, Ito S, Shigematsu M, Sakka S, Yamamuro T. Fatigue and life-time of bioactive glass-ceramic A–W containing apatite and wollastonite. J Mater Sci 1987;22:4067–70.
[22] Bohner M, Lemaitre J. Can bioactivity be tested in vitro with SBF solution? Biomaterials 2009;30:2175–9.
[23] Jonasova L, Müller FA, Helebrant A, Strnad J, Greil P. Hydroxyapatite formation on alkali-treated titanium with different content of Na^+ in the surface layer. Biomaterials 2002;23:3095–101.
[24] Jonasova L, Müller FA, Helebrant A, Strnad J, Greil P. Biomimetic apatite formation on chemically treated titanium. Biomaterials 2004;25:1187–94.
[25] Muller L, Muller FA. Preparation of SBF with different HCO_3-content and its influence on the composition of biomimetic apatite on anodic TiO_2 nanotubes. Acta Biomater 2005;2:181–9.